Ultrasound Sensing with a Photonic Crystal Slab

Eric Y. Zhu[1,2,*], **Cory Rewcastle**[1,2], **Raanan Gad**[1,2], **Li Qian**[1], **Ofer Levi**[1,2]
[1] *Department of Electrical and Computer Engineering, University of Toronto, 10 Kings College Road, Toronto, Ontario M5S 3G4, Canada*
[2] *Institute of Biomaterials and Biomedical Engineering, University of Toronto, 164 College Street, Toronto, Ontario M5S 3G9, Canada*
**Corresponding author: eric.zhu@utoronto.ca*

Abstract: We experimentally demonstrate a compact architecture for ultrasound acoustic sensing based upon a photonic crystal slab (PCS) fabricated on top of a thin mechanically pliable silicon substrate. A noise-equivalent pressure of 2.0 kPa (0.072 kPa/$\sqrt{\text{Hz}}$) at 5 MHz is observed.

OCIS codes: (350.4238) Nanophotonics and photonic crystals; (110.7170) Ultrasound

Acoustic sensing is a technology with myriad applications, ranging from biomedical imaging to non-destructive testing (NDT). The common workhorse for such applications is the piezoelectric transducer [1], which use the piezoelectric effect to both transmit and receive ultrasound signals. However, these devices suffer from narrow bandwidths, and poor sensitivity. Recently, work on capacitive micromachined ultrasound transducers (cMUTs), which are fabricated using CMOS-compatible technology, has helped to improve signal detection bandwidths. However, the detection and generation of ultrasonic signals are still performed electrically. When placed into an array, both piezoelectric and cMUT devices experience significant electrical crosstalk [2], as well as electromagnetic interference (EMI) in general.

One solution to eliminating cross-talk and EMI is to detect the acoustic signals optically. Such implementations often couple the optical and acoustic signals using an optical cavity. The changes in the dimensions of the optical cavity due to the acoustic signal is then imprinted upon the optical reflectivity. Recently, Fabry-Perot devices [3] demonstrated a noise-equivalent pressure of 90 μPa/$\sqrt{\text{Hz}}$ at 2.5 kHz, but sensitivity at ultrasonic frequencies ($>$1 MHz) was not demonstrated. Pi-phase-shifted fiber Bragg gratings (FBG) [4] have been shown to have kPa level sensitivity in the ultrasound regime, but fabricating an FBG sensor array with milimetre spacing remains difficult.

Here, we demonstrate a compact architecture for a photonic crystal slab (PCS) sensor that is capable of detecting ultrasonic acoustic signals. Similar slab sensors were previously used for refractive-index sensing [5]. The device is fabricated using CMOS-compatible technology. A cross-section of the device is shown in Fig. 1a. A 500-μm-thick silicon wafer with thermal oxide and stoichiometric Si_3N_4 layer grown on top is used. Circular membranes of diameters 100 to 300 microns is patterned into the silicon layer (back side) using a dry Bosch etch, leaving behind only a 10-micron layer of silicon that deforms under acoustic excitation. A PCS structure is patterned on the nitride layer (front side) of the device through e-beam lithography. The nanohole radius (r = 150 nm) and pitch (a = 1.05 μm) are chosen so that a TE-like Fano resonance peak appears at about 1526 nm (Fig. 1b). The slab structure consists of a 300 $\times$ 300 array of nanoholes, centered about the Si membrane. An array of these PCS/membrane combinations are fabricated on a 15 mm $\times$ 15 mm wafer (Fig. 2a inset), with sensor spacings of 1 mm.

The experimental setup is shown in Fig. 2a. The back side of the structure is immersed in water, while the front side is kept dry using a custom holder. At a distance of 12 cm beneath the silicon membrane is an ultrasound (U/S) transducer (Panametrics C326) with a center frequency of 5 MHz and active element diameter of 9.6 mm. The output of the transducer has been calibrated with an Onda HMB-0200 hydrophone.

Light from a narrow linewidth tunable laser source is used to interrogate the PCS. An f = 8 mm asphere out-

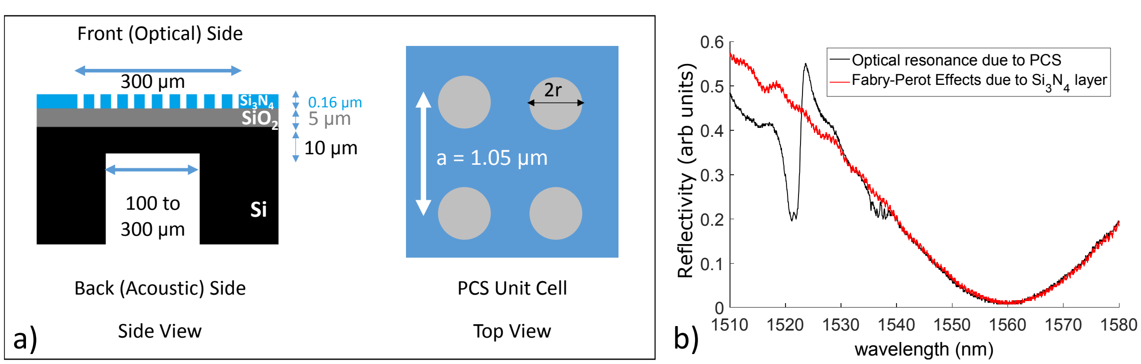

Fig. 1. a) Device geometry. The back side of the sensor consists of a thin membrane of silicon that is mechanically pliable. The front side of the sensor is composed of a photonic crystal slab (PCS) consisting of nanoles in Si_3N_4. b) The optical reflectivity for the PCS shows a peak at 1526 nm (black trace). Fitting to a Fano lineshape reveals a characteristic width of 2.2 nm, giving us a Q-factor of 690. The red trace shows the reflectivity from an unpatterned portion of the Si_3N_4 layer.

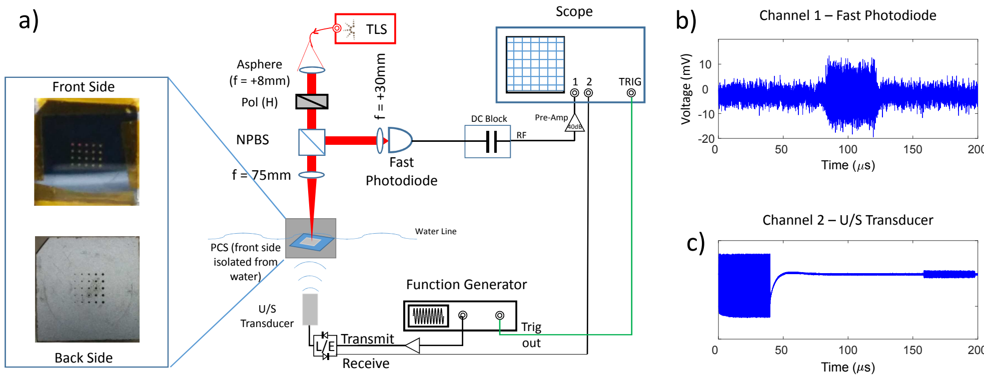

Fig. 2. a) Experimental setup. See text for details. The inset shows the physical chip on which a 2D array of 4×5 PCS sensors are present, each separated by 1 mm. On the back side, there are 5 columns of membranes; the leftmost (rightmost) column contains membranes of diameter 100 μm (300 μm). b) The optical reflectivity of the PCS is monitored with a fast photodiode and oscilloscope. Notice that the tone burst is observed at 80 μs. c) The transmitted and back-reflected acoustic signals picked up by the ultrasound (U/S) transducer are routed appropriately using an L/E (limiter/expander) circuit. The reflected signal arrives at 160 μs, twice as long as it takes the signal to arrive at the PCS.

couples and collimates the laser light from a fiber, and an $f = 75$ mm planoconvex lens creates a 150 μm diameter spot size on the slab. The backreflected beam is redirected through a non-polarizing beam splitter (NPBS) to a fast photodiode, whose RF output is then amplified (voltage gain of ~200), and fed into an oscilloscope.

The ultrasound transducer is driven with 5 MHz sinusoidal tone bursts consisting of 200 periods, at varying voltage amplitudes. The maximum amplitude used allows for the generation of pressure waves with peak-to-peak values of up to 80 kPa at a distance of 12 cm away, and an acoustic beam diameter (FWHM) of 3.7 mm. Figure 2b shows an observed time series as measured by the fast photodiode, after 64 averages (for a total integration time of 2.56 ms). An RMS voltage can be extracted from the trace. Similar traces can be obtained at varying pressures, and the RMS voltage for each can obtained. For two different membrane diameters (200 and 300 μm), the applied pressure is varied, and the RMS voltage measured. The results are plotted in Fig. 3a, demonstrating a linear response. The 300 μm membrane is four times as sensitive as the 200 μm, with a noise-equivalent pressure (NEP) of 2.0 kPa (0.072 kPa/$\sqrt{\mathrm{Hz}}$).

Figure 3b shows the acoustic sensitivity of the 300 μm device as a function of wavelength; the acoustic sensitivity of the PCS correlates well with the slope of the resonance. This measurement acts as a check that the PCS structure contributes primarily to our ability to measure the acoustic waves; the optical response is caused by the mechanical deformation of the membrane and PCS structure in response to the impinging acoustic waves. We anticipate further sensitivity improvements when the front side PCS surface is immersed in water, as pressure-induced index of refraction changes would then be readily observed by the PCS [5], providing another mechanism for acoustic sensing.

In summary, we have demonstrated a compact optical PCS-based ultrasound sensor. It consists of an optical resonator (the PCS) patterned above a mechanically pliable and acoustically sensitive silicon membrane. A noise equivalent pressure of 0.072 kPa/$\sqrt{\mathrm{Hz}}$ was observed for the device when detecting 5 MHz ultrasonic waves.

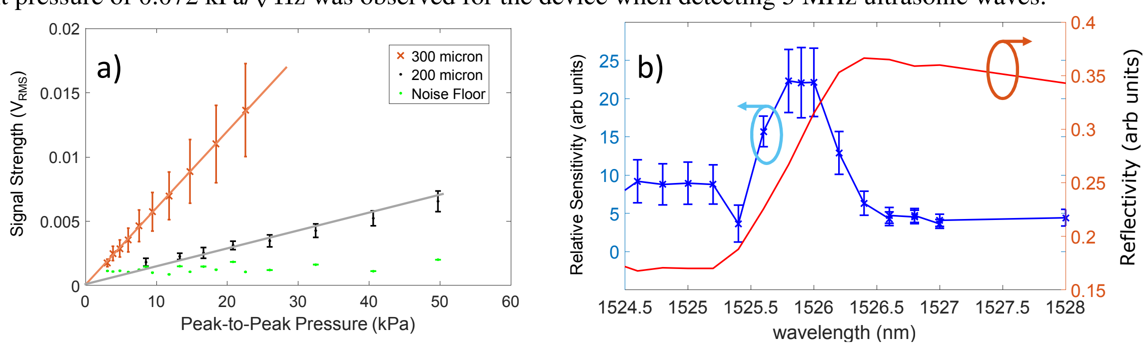

Fig. 3. a) Measured acoustic sensitivity at varying pressures for two different-sized membranes. The 300 μm diameter device yields a four-fold improvement over the 200 μm device. b) The acoustic sensitivity of the sensor is measured as a function of wavelength. The sensitivity (blue curve) is maximized when the slope of the resonance reflectivity (red curve) is maximized.

References

1. A. Webb and G. C. Kagadis, Medical Physics **30**, 2267–2267 (2003).
2. B. Bayram, M. Kupnik, G. G. Yaralioglu, et al., IEEE transactions on ultrasonics, ferroelectrics, and frequency control **54** (2007).
3. C. Jan, W. Jo, M. J. Digonnet, and O. Solgaard, et al., IEEE Photonics Technology Letters **28**, 123–126 (2016).
4. G. Wissmeyer, D. Soliman, R. Shnaiderman, A. Rosenthal, and V. Ntziachristos, Opt. Lett. **41**, 1953–1956 (2016).
5. C. Nicolaou, W. T. Lau, R. Gad, H. Akhavan, R. Schilling, and O. Levi, Optics express **21**, 31698–31712 (2013).